life

MDPI

Article

Dietary α-Linolenic Acid Enrichment Is Associated with p38 Mapk/FoxO1-Related Signaling and Improved Fillet Quality in Nile Tilapia (*Oreochromis niloticus*)

Fang Chen [1,2,†], Hangbo Zhu [1,†], Ziying Mo [1], Yuanyou Li [1] and Dizhi Xie [1,*]

[1] College of Marine Sciences, South China Agricultural University, Guangzhou 510642, China
[2] Institute of Eco-Environmental Research, Guangxi Academy of Sciences, Nanning 530007, China
* Correspondence: xiedizhi@scau.edu.cn
† These authors contributed equally to this work.

Simple Summary

Improving the nutritional value and texture of tilapia fillets is important for enhancing their quality and consumer acceptance. This study investigated whether increasing dietary α-linolenic acid (ALA), a plant-derived omega-3 fatty acid, could improve fillet quality in Nile tilapia and explored the potential underlying mechanisms. Fish fed an ALA-enriched diet for eight weeks exhibited a more favorable muscle fatty acid composition, including higher levels of beneficial omega-3 fatty acids, alongside improvements in several texture characteristics. These changes were accompanied by increased muscle fiber density and a greater proportion of smaller muscle fibers. Further molecular and cell-based analyses suggested that ALA may influence muscle development and protein degradation through pathways involving p38 MAPK and FoxO1. Although further investigation is needed to confirm these mechanisms, the results suggest that adjusting dietary lipid composition may be a promising nutritional strategy for improving the nutritional quality and texture of farmed Nile tilapia fillets.

Abstract

Farmed tilapia fillets are often perceived as having poor eating quality due to their soft texture and low content of n-3 long-chain polyunsaturated fatty acids (LC-PUFA). Dietary α-linolenic acid (ALA) has been proposed as a potential strategy to improve these characteristics, although the underlying mechanism remains unclear. Juvenile Nile tilapia (*Oreochromis niloticus*) were fed either a soybean-oil-based diet (D1, 0.58% ALA) or a soybean-oil/linseed-oil diet (D2, 1.35% ALA) for 8 weeks, followed by analyses of muscle quality, transcriptomic profiles, and cell responses. The results demonstrated that growth performance and muscle proximate composition did not differ significantly between treatments, whereas condition factor was significantly higher in the D2 group. Compared with D1, D2 was associated with an increase in n-3 PUFA proportion from 8.05% to 23.71% and a 1.97-fold increase in LC-PUFA, along with reductions in n-6 PUFA (−24.3%) and saturated fatty acids (−11.6%). Six texture attributes measured, namely hardness, chewiness, gumminess, springiness, resilience and cohesiveness were higher in D2 fish, whereas adhesiveness did not differ significantly between treatments. D2 fish also exhibited higher muscle fiber density and a greater proportion of small-diameter fibers. Transcriptomic analysis identified 207 differentially expressed genes (24 upregulated and 183 downregulated) enriched in pathways related to cardiac muscle contraction, adrenergic signaling,

Academic Editor: Einar Ringø

Received: 23 September 2026
Revised: 5 November 2026
Accepted: 9 November 2026
Published: 12 November 2026

Copyright: © 2026 by the authors. Licensee MDPI, Basel, Switzerland. This article is an open access article distributed under the terms and conditions of the Creative Commons Attribution (CC BY) license.

lipid metabolism and FoxO signaling. Network analysis grouped the sarcomeric/myogenic and atrophy-related genes (*mstn, foxo1, p38 mapk, mkk4*) into two inversely correlated modules, with *foxo1* emerging as the most highly connected gene. Muscle qPCR confirmed the up-regulation of *myod* and *myf5* and the down-regulation of *mstn*, *p38 mapk* and *foxo1* in D2 fish. In myoblasts, ALA increased cell viability and myogenic factor expression while suppressing *p38 mapk* and *foxo1*, and these effects were attenuated by hesperetin. Overall, the ALA-enriched dietary lipid formulation was associated with a more favorable muscle fatty acid profile and texture characteristics in Nile tilapia. The cell-based findings further suggest the potential involvement of p38 Mapk/FoxO1-related signaling, although its causal role requires further validation.

Keywords: α-linolenic acid; myocyte viability; muscle texture; Nile tilapia

1. Introduction

Aquaculture has become the principal source of aquatic animal food for human consumption. According to the latest global assessment, total fisheries and aquaculture production reached a record 235 million tonnes in 2024, and aquaculture production of aquatic animals exceeded 100 million tonnes for the first time, supplying 53% of total aquatic animal production and more than 59% of the aquatic animal food production intended for human consumption [1]. This rapid expansion, however, has been accompanied by concerns regarding product quality in certain intensively farmed species. For instance, under high-density rearing and diets heavily reliant on plant oils, farmed fillets frequently exhibit a softer texture and lower n-3 long-chain polyunsaturated fatty acids (LC-PUFA) levels [2]. Nile tilapia (*Oreochromis niloticus*) is one of the most economically important freshwater aquaculture species, owing to its high productivity, environmental resilience, broad dietary adaptability and low feed requirements [3,4]. However, intensive farming practices, particularly high stocking densities and the use of soybean-oil-based diets, may compromise its fillet quality, contributing to reduced muscle firmness and chewiness, as well as low levels of n-3 LC-PUFA [5,6]. These limitations may negatively affect the nutritional value and consumer acceptability of farmed tilapia. Although substantial progress has been made in improving aquaculture productivity, enhancing fillet quality remains an important challenge. Therefore, developing effective strategies to simultaneously improve the nutritional value and the texture properties of tilapia fillet is of considerable practical significance.

The accumulation of n-3 LC-PUFA in farmed tilapia tissues depends on two major sources: direct dietary intake of preformed n-3 LC-PUFA from fish oil, fish meal or algal oil, and endogenous biosynthesis from α-linolenic acid (ALA, 18:3n-3) [7]. Tilapia possess a complete enzymatic complement for LC-PUFA biosynthesis, with substantial biosynthetic capacity in the liver and intestine. Consequently, ALA-rich diets may enhance n-3 LC-PUFA deposition in skeletal muscle [7]. Beyond their contribution to tissue fatty acid composition, dietary lipids can also act on muscle quality. For instance, a blend of rapeseed and palm oils improved muscle texture compared with soybean oil in golden pompano fed low-fish-oil diets [8]. Similarly, early provision of linseed oil reprogrammed lipid metabolism and increased muscle n-3 LC-PUFA in juvenile Nile tilapia [9]. Muscle texture is a composite trait influenced by muscle fiber density and diameter, as well as the abundance and cross-linking of intramuscular collagen [2]. Previous studies have demonstrated that muscle texture can be modulated by dietary nutrients, including histidine, glycine, proline, hydroxyproline and faba bean [10–12], and is also sensitive to changes in

the animals' energy status [13]. Collectively, these findings indicate that cultured fish muscle exhibits considerable physiological plasticity, highlighting the potential of nutritional strategies to simultaneously improve muscle texture and n-3 LC-PUFA accumulation.

The myogenic program underlying this plasticity is regulated by the myogenic regulatory factors, including Myod, Myf5, Myf4 and Myog, which are involved in myoblast proliferation and differentiation, and by their antagonist myostatin (Mstn) [14], within a complex signaling network that integrates nutritional and hormonal signals [15]. FoxO1 has been implicated as a negative regulator of myogenic gene expression, including the repression of *myod*, *myog* and *myf5*, and the induction of *mstn*, although its functions may vary with the cellular context [16,17]. p38 Mapk signaling can modulate FoxO1 function in certain cellular contexts and contributes to different stages of myogenesis [18]. However, its effects are isoform-dependent: p38α generally promotes cell-cycle exit, myogenic differentiation and myotube formation, whereas p38γ can support the proliferation of myogenic precursor cells by preventing premature differentiation [19]. Thus, the biological effects of p38 Mapk signaling depend on the specific isoform, developmental stage and cellular context, and pathway activity cannot be inferred from transcript abundance alone. In fish, DHA has been reported to promote myofiber development in blunt snout bream by activating AMPK/Sirt1 signaling [20] and enhance textural firmness in common carp by restraining the FoxO1-related pathway [21]. However, whether dietary lipid formulations enriched in ALA are associated with changes in myogenic gene expression, including p38 Mapk/FoxO1-related transcriptional responses, in fish muscle remains unclear.

In our previous work, tilapia fed a high-ALA diet exhibited an improved muscle texture and an increased fillet n-3 LC-PUFA content [7,22]; however, the regulatory mechanism underlying these changes remains unclear. The present study therefore combined four levels of analysis: (i) growth performance, fillet proximate and fatty acid compositions, edible quality and texture, and muscle histology of tilapia fed two diets differing in lipid formulation (ALA, 8.42% vs. 35.78% of total fatty acids); (ii) RNA sequencing of the muscle transcriptome to identify the differentially expressed genes (DEGs) and the enriched pathways; (iii) a gene–gene Pearson correlation network built on the DEGs together with an exploratory correlation-network analysis to prioritize candidate regulators for subsequent validation [23,24]; and (iv) validation in a myoblast cell model, in which ALA was applied alone and in combination with a p38 Mapk agonist to test whether the pathway is required for the ALA effect [25,26]. We hypothesized that dietary ALA is associated with improvement in the nutritional value and the texture of tilapia fillets, potentially accompanied by changes in myogenic gene expression and the p38 Mapk/FoxO1-related pathway. This study also aimed to explore the potential involvement of this signaling pathway in ALA-associated changes in myoblast viability. The results may provide a mechanistic basis and a practical dietary strategy for improving the quality of farmed tilapia.

2. Materials and Methods

2.1. Experimental Diets and Feeding Trial

Soybean oil and linseed oil were utilized as lipid sources, while rapeseed meal and soybean meal were employed as protein sources. Two experimental diets were formulated to contain similar crude lipid (10%) and crude protein (32%) contents, but differed in their lipid sources and fatty acid profiles: Diet D1 included soybean oil as the lipid source, whereas Diet D2 contained a mixture of soybean oil and linseed oil as lipid sources, with linseed oil replacing 5% of the diet (*w*/*w*) otherwise supplied by soybean oil. According to the fatty acid profiles presented in Table S1, α-linolenic acid (ALA, C18:3n-3) accounted for 8.42% and 35.78% of total fatty acids in D1 and D2, respectively, while linoleic acid (LA, C18:2n-6) accounted for 51.33% and 30.98%, respectively. Thus, the two diets

differed in their overall fatty acid compositions rather than exclusively in ALA content. The ingredient compositions, proximate analyses, and fatty acid profiles of the experimental diets are presented in Table S1. Diet preparation and storage followed the previously established procedures by our research group [7].

The juvenile tilapia (initial weight ~4.3 g) were procured from a nearby hatchery and underwent a 14-day acclimation period at the aquaculture systems at South China Agricultural University. The fish were reared in pond floating cages (1.0 m × 1.0 m × 1.5 m). Before commencing the experiment, a total of 280 fish with comparable initial body weight (~ 10.1 g) were stochastically distributed into 8 cages, with 35 fish per cage. Each dietary treatment was allocated to four separate cages. Throughout the 8-week feeding trial, the fish were fed twice daily (at 9:00 and 17:00) until apparent satiation. Feeding was stopped when the fish no longer aggregated at the feeding area and active feeding ceased, which was considered apparent satiation. Feed was weighed before each feeding, and the remaining feed was weighed after feeding. The difference was recorded as the feed intake of each cage. Water quality was maintained at a pH of approximately 7.2, a water temperature of 26 ± 3 °C, and a dissolved oxygen concentration of 6.0–6.5 mg/L.

2.2. Sample Collection and Assessment of Growth Performance

After an 8-week feeding period, the fish were sampled following a 24-h fasting duration. Subsequently, all fish in each cage were anesthetized with MS-222 (100 mg/L, Sigma-Aldrich, St. Louis, MO, USA), counted and weighed. These data were used to calculate the weight gain rate (WGR), specific growth rate (SGR), and survival rate (SUR) [7].

To reduce the number of fish sacrificed, three fish were randomly selected from each cage (12 fish per group). These fish were weighed, and body length was measured, and the fish were dissected. The viscera and liver were separated and weighed for the calculation of condition factor (CF), hepatosomatic index (HSI), and viscerosomatic index (VSI) [7]. For muscle sampling, a dorsal muscle sample from one side was cut into approximately 0.5 cm segments and fixed in 10% buffered formalin for histological examination. The remaining muscle from the same side was used for analysis of muscle proximate composition, while muscle from the other side was used for texture analysis. Additionally, muscle samples were collected from three other fish in each cage (12 fish per group), flash-frozen in liquid nitrogen, and stored at −80 °C for fatty acid, gene expression, and transcriptome analyses.

2.3. Analysis of Proximate and Fatty Acid Compositions

The diets and muscle samples were analyzed for their proximate composition using established methodologies [27]. In brief, the crude lipid content was determined by employing the Soxhlet extraction technique. The evaluation of crude protein content involved measuring the total nitrogen (N) levels using the Kjeldahl method following acid digestion, and the crude protein percentage was calculated as % N × 6.25. Moisture content was determined by drying the samples in an oven at 80 °C until a constant weight was achieved. Ash content was determined by incinerating the samples in a muffle furnace at 550 °C for 6 h.

Dietary and muscle fatty acid compositions were analyzed following the procedure outlined by Li et al. [28]. Briefly, a combination of chloroform and methanol (2:1, *v*/*v*) with the addition of 0.01% butylated hydroxytoluene (BHT) was utilized to extract lipids from the experimental diets and fish fillets. Fatty acid methyl esters (FAME) were obtained by subjecting the total lipid to boron trifluoride diethyl etherate (approximately 48%, Acros Organics, Waltham, MA, USA), followed by analysis using gas chromatography (GC-2010 plus; Shimadzu, Kyoto, Japan). Individual FAMEs were determined by comparing them

with commercially available standards (Sigma, St. Louis, MO, USA) and measured using the CLASS-GC2010-plus workstation (Shimadzu).

2.4. Analysis of Muscle Edible Qualities and Texture

Muscle quality was evaluated by measuring cooking loss (CL), water loss (WL), and textural properties. For CL determination, pre-weighed muscle samples were immersed in boiling water (100 °C) for 5 min, and the samples were wrapped in filter paper and subjected to a 1-kg load for 5 min. Both CL and WL were calculated as the percentage reduction in sample weight relative to the initial weight. The textural properties, including springiness, hardness, chewiness, resilience, adhesiveness, cohesiveness, and gumminess, were assessed utilizing a universal Texture Analyzer (Universal TA, Shanghai Turnkey Pull, Shanghai, China). Dorsal muscle samples were prepared into uniform pieces (2 × 2 × 0.5 cm) and stored at 4 °C for 24 h before analysis at room temperature. Texture measurements were performed using a cylindrical probe (5 mm in diameter) at a compression speed of 0.8 mm/s and a deformation of 60% of the original sample thickness. Each sample was tested twice, with a 30-s interval between measurements. The specific procedures used for this analysis were adapted from Ma et al. [29].

2.5. Quantitative Histological Analysis

Muscle tissue samples were collected from the dorsal region of each fish and fixed in 10% buffered formalin for 24 h. The fixed tissues were subsequently dehydrated through a graded ethanol series, cleared in xylene, embedded in paraffin, and transversely sectioned at a thickness of 5 um, following the method described by Valente et al. [30]. The sections were stained with hematoxylin and eosin (H&E), and examined using an optical microscope (Eclipse 80i, Nikon, Tokyo, Japan). Images were acquired using a Nikon digital imaging system equipped with a DS-U2 camera (Tokyo, Japan). For histological analysis, three sections per fish were examined, with five randomly selected, non-overlapping fields analyzed per section at ×400 magnification. Muscle fiber morphometry was conducted utilizing Image J software (Version 1.54g, National Institutes of Health, Bethesda, MD, USA). Muscle fibers with clearly defined boundaries were selected for measurement, and fiber diameters were determined according to Almeida et al. [31]. Approximately 200 muscle fibers per fish were analyzed. The measurements were averaged at the appropriate biological-replicate level before subsequent statistical analysis.

2.6. Transcriptome Sequencing and Analysis

The muscle transcriptome of the two dietary groups was profiled to identify the transcriptional basis underlying the observed phenotypic differences. For each group, total RNA was isolated from the white muscle of three fish per cage, and these three fish were pooled into one sample. To reduce sequencing costs, three out of the four cages per diet were randomly selected, yielding six independent sequencing libraries (n = 3 per group). Following mRNA enrichment using oligo(dT) magnetic beads and fragmentation, double-stranded cDNA was synthesized using a SuperScript cDNA synthesis kit (Invitrogen, Carlsbad, CA, USA). The cDNA fragments were end-repaired, phosphorylated, A-tailed, and ligated to sequencing adapters. Fragments of 200 bp–300 bp were size-selected using 2% Low Range Ultra Agarose, and amplified for 15 cycles with Phusion high-fidelity DNA polymerase (New England Biolabs, Boston, MA, USA). Library quantity was determined on a TBS380 fluorometer, and paired-end reads (150 bp) were generated on an Illumina NovaSeq 6000 platform (Illumina, San Diego, CA, USA) by Shanghai Majorbio Bio-pharm Technology Co., Ltd. (Shanghai, China).

Raw sequencing reads were processed with SeqPrep (v1.2) and Sickle (v1.3.3) to remove adaptor-contaminated reads, reads containing more than 10% ambiguous bases,

and reads with quality scores lower than 20 for more than 50% of their bases. Sequencing quality was evaluated based on raw and clean read counts, Q20 and Q30 percentages, and GC content. Across the six libraries, 42.66 to 77.34 million clean reads were obtained per sample, with Q30 values ranging from 95.57% to 96.84%. The clean reads were aligned to the Nile tilapia reference genome (GCF_001858045.2) with HISAT2 (v2.2.1), based on default parameters. The overall and uniquely mapped read percentages were 63.26% to 96.5% and 58.94% to 83.75%, respectively. Detailed sequencing quality and mapping statistics for each library are provided in Table S3.

Transcript and gene abundances were quantified with RSEM (v1.3.3) using the corresponding genome annotation, with gene-level read counts used for differential expression analysis and transcripts per million (TPM) values used to describe expression levels. Differentially expressed genes (DEGs) between the D1 and D2 groups were identified using DESeq2 (v1.40.2) in R, with an absolute $\log_2$ fold change of ≥1 and a Benjamini–Hochberg-adjusted p value < 0.05 as the significance thresholds. Differential expression statistics reported in Table S4 ($\log_2$ fold change, Wald-test p value and Benjamini–Hochberg-adjusted p value, padj) are taken from this DESeq2 fit, with $\log_2$ fold changes expressed as $\log_2$(D1/D2) so that positive values indicate lower abundance in the D2 group, and independent filtering was applied by DESeq2 as implemented by default. TPM values are reported for descriptive purposes only and were not used for significance testing.

Functional enrichment analyses were performed using Gene Ontology (GO) and Kyoto Encyclopedia of Genes and Genomes (KEGG) annotations. The background gene sets for GO and KEGG enrichment analyses comprised all annotated genes in the Nile tilapia reference genome. Enrichment significance was assessed using a hypergeometric test followed by Benjamini–Hochberg correction, with adjusted $p < 0.05$ regarded as significant. The 15 most significantly enriched GO terms and KEGG pathways were displayed as bubble plots, with bubble size and colour representing DEG counts and adjusted p value, respectively. The rich factor is defined as the ratio of DEGs among all background genes annotated to each term or pathway.

2.7. Correlation Analysis of Differentially Expressed Genes and Prioritisation of Candidate Genes

Pairwise Pearson correlation coefficients among the GO/KEGG-filtered genes were computed from $\log_2$(TPM + 1) values of six samples (three biological replicates each of D1 and D2). Genes were ordered by average-linkage hierarchical clustering of the $1 - r$ distance matrix with optimal leaf ordering, and visualized in a diverging blue–white–red heatmap (blue, $r = -1$; white, $r = 0$; red, $r = +1$) in which coefficients with $|r| \geq 0.70$ are annotated in the cells. Genes were ranked by a hub score defined as the mean $|r|$ with all other genes, and the top five were taken as prioritized candidates. With $n = 6$, $|r| > 0.811$ indicates $p < 0.05$ (two-tailed). Analyses were conducted in Python 3.13 (pandas, NumPy, SciPy, Matplotlib). Because the genes were pre-selected on the basis of differential expression and only six samples were available, this analysis was treated as exploratory and hypothesis-generating; the coefficients and the ranking are not stable estimates, and no causal or hierarchical inference is made from them.

2.8. Myoblast Culture and Treatment with ALA and Hesperetin

The common carp myoblast line used here was kindly provided by Prof. Nie (Henan Normal University), as no tilapia myoblast line was available to us at the time of the experiment. Cells were maintained following Zhi et al. [32] at 28 °C under 5% CO_2 in DMEM/F12 (Gibco, Life Technologies, Grand Island, NY, USA) supplemented with 10% FBS (Gibco, Life Technologies, Grand Island, NY, USA), 100 IU/mL streptomycin and 100 U/mL penicillin (Beyotime, Shanghai, China).

Two experimental treatments were performed using myoblasts cultured in DMEM/F12 supplemented with 5% fetal bovine serum (FBS) until approximately 80% confluent. To examine the concentration-dependent effects of ALA, cells seeded in 12-well plates (10^6 cells/well) were switched to serum-free induction medium (DMEM/F12) containing ALA–BSA complexes at final concentrations of 0, 50 and 100 μM (ALA, Sigma, USA; complexed with fatty-acid-free bovine serum albumin (BSA, Cayman Chemical, Ann Arbor, MI, USA) in 10% BSA solution and stored at −20 °C; the 0 μM group received BSA vehicle alone). To explore the potential involvement of p38 Mapk/FoxO1-related signaling in ALA-associated cellular responses, cells seeded in six-well plates (10^6 cells/well) were transferred to induction medium (DMEM/F12) containing ALA–BSA complexes (50 μM) with or without 400 μM hesperetin (Hes, p38 Mapk agonist; MCE, China; dissolved in dimethyl sulfoxide (DMSO) and stored at 4 °C), with DMSO-treated cells as controls. After 12 h, cell morphology was imaged, cells were harvested by trypsinization, and total RNA was isolated using TRIZOL reagent (Invitrogen, USA).

2.9. Analysis of Cell Viability

According to the previous study [32], cell viability-associated metabolic activity was measured using a Cell Counting Kit (CCK-8, Beyotime, China). Briefly, following the incubation of the fatty acid and agonist, CCK-8 solution (80 μL/well) was introduced, and the cells were incubated at 28 °C for 4 h. The microplate reader was employed to determine the absorbance at 450 nm for each well. The relative cell viability was expressed as follows: Relative cell viability (%) = [(OD incubation − OD blank)/(OD control − OD blank)] × 100%. The CCK-8 assay was used as an indirect indicator of viable cell metabolic activity rather than a direct measure of cell proliferation.

2.10. Analysis of Real-Time Quantitative PCR

Total RNA was extracted from muscle samples and myoblasts using a Tissue Total RNA Extraction Kit (Bioflux, Tokyo, Japan) according to our previously described procedure [7]. RNA concentration and purity were determined using a Nanodrop, and 1 μg of total RNA was reverse-transcribed into cDNA using a FastKing gDNA Dispelling RT Supermix (TIANGEN Biotech, Beijing, China) according to the manufacturer's instructions.

Quantitative real-time PCR (qPCR) was performed using SYBR Green to measure the relative mRNA expression levels of genes involved in muscle development (*myod*, *myog*, *myf4*, *myf5*, *mstn*, *p38-mapk*, and *foxo1*) in muscle and myoblasts. The primer sequences were listed in Table S2. Cycling conditions were 95 °C for 30 s, followed by 40 cycles of 95 °C for 5 s and 60 °C for 30 s, with fluorescence acquired at the end of each cycle, and a final melt curve from 60 to 95 °C. Amplification efficiencies, calculated from the slope of standard curves generated from five 10-fold serial dilutions of pooled cDNA, ranged from 95% to 105% for all primer pairs (Table S2). A single melting peak was observed for each primer pair, confirming amplification specificity.

The stability of candidate reference genes was assessed with geNorm (M value) and NormFinder across all samples, and the most stable genes were used for normalisation: β-actin for Nile tilapia muscle and 18S rRNA for common carp myoblasts. Relative gene expression was calculated using the $2^{-\Delta\Delta CT}$ method after confirming that the amplification efficiencies of the target and reference genes were comparable. For the Nile tilapia, four independent cages per treatment were regarded as biological replicates (n = 4); for the myoblast experiment, three independently conducted experiments were regarded as biological replicates (n = 3). Each biological sample was analyzed in three technical qPCR replicates, and the mean Ct value of the technical replicates was used to represent that biological sample for subsequent analysis. Technical replicates were not treated as independent biological replicates.

2.11. Statistical Analysis

All data are presented as mean ± standard error of the mean (SEM). In the feeding trial, the cage was considered the experimental unit (n = 4 per dietary treatment). The 12 fish per group (3 fish per cage × 4 cages) were treated as subsamples rather than independent biological replicates, and their measurements were averaged within each cage before statistical analysis. For transcriptomic analysis, one library was prepared per cage, with three cages analyzed per dietary treatment (n = 3).

Before parametric analyses, data were assessed for normality using the Shapiro–Wilk test and for homogeneity of variances using Levene's test. Comparisons between the two dietary treatments in the feeding trial were performed using an independent-samples t-test. To assess the quantitative agreement between RNA-seq and qPCR data, the $\log_2$ fold-change ($\log_2$FC) values of the selected genes obtained from both methods were compared using Pearson correlation analysis. RNA-seq $\log_2$FC was calculated as $\log_2$(mean TPM in D2/mean TPM in D1) from three biological replicates per group, and qPCR $\log_2$FC was calculated from the corresponding group means after normalization of the D1 group to 1.00. The coefficient of determination (R^2) and Lin's concordance correlation coefficient (CCC) were also calculated to evaluate the strength and concordance of the linear relationship. Statistical significance was set at $p < 0.05$. These statistical analyses and data visualizations were performed using Python (version 3.9) with the SciPy and pandas libraries.

For the ALA dose experiment, data were analyzed using one-way analysis of variance (ANOVA) followed by Tukey's multiple-comparison test (n = 3 independent experiments; replicate wells within each experiment were averaged as technical replicates). For the ALA × hesperetin experiment, data were analyzed using two-way ANOVA, with ALA and hesperetin as fixed factors and their interaction included in the model. When a significant interaction was detected, simple-effects analyses were performed, followed by Tukey-adjusted pairwise comparisons when appropriate. When the interaction was not significant, the main effects were interpreted, and pairwise comparisons of marginal means were performed for significant main effects, with appropriate adjustment for multiple comparisons. Significant differences were indicated by different letters in the corresponding figures, according to the comparisons performed. Statistical analyses were conducted using IBM SPSS Statistics for Windows, version 20.0 (IBM Corp., Armonk, NY, USA). Differences were considered statistically significant at $p < 0.05$.

3. Results

3.1. Growth Performance

The growth performance of tilapia is presented in Table 1. There were no significant differences observed between the two dietary groups ($p > 0.05$) in terms of SGR, FCR, WGR, SUR, HSI and VSI. While CF of fish fed diets D2 was significantly higher than that of those fed diets D1 ($p < 0.05$).

Table 1. Growth performance of tilapia fed the two different diets.

	Dietary Groups	
	D1	**D2**
IBW	10.13 ± 0.06	10.09 ± 0.07
FBW	115.85 ± 5.83	113.94 ± 6.07
WGR (%)	1043.65 ± 32.25	1029.35 ± 21.40
SGR (%)	4.35 ± 0.09	4.33 ± 0.05
FCR	1.11 ± 0.05	1.12 ± 0.01
SUR (%)	100	100

HSI (%)	0.68 ± 0.05	0.65 ± 0.06
VSI (%)	9.97 ± 0.35	10.03 ± 0.35
CF (g cm^{-3})	3.52 ± 0.06 [b]	3.85 ± 0.11 [a]

Note: IBW, initial body weight; FBW, final body weight; SGR, specific growth rate; FCR, feed conversion ratio; WGR, weight gain rate; HSI, hepatosomatic index; VSI, viscerosomatic index; CF, condition factor. Results are presented as the mean ± SEM (n = 4). Values in each row without sharing a common letter are significantly different ($p < 0.05$).

3.2. Muscle Proximate and Fatty Acid Compositions, Edible Quality, and Texture

The proximate compositions and fatty acid profiles of muscle samples are presented in Table 2. The analysis revealed no significant differences in muscle moisture, protein, or lipid between the two dietary groups ($p > 0.05$). Noticeable differences in muscle fatty acid compositions were observed between the two dietary groups. The D2 group exhibited significantly higher levels of n-3 PUFA and LC-PUFA ($p < 0.05$), with a 1.97-fold increase in LC-PUFA content compared to the D1 group. Conversely, the proportions of n-6 PUFA and SFA were 24.30% and 11.57% lower, respectively, in comparison to those observed in the D1 group.

Table 2. Muscle proximate and fatty acid compositions of tilapia fed different diets.

	Dietary Groups	
	D1	**D2**
Proximate composition (%)		
Moisture	77.35 ± 0.51	77.17 ± 0.15
Crude protein	88.41 ± 0.73	88.91 ± 0.75
Crude lipid	3.76 ± 0.23	4.04 ± 0.37
Main fatty acid compositions (% total fatty acid)		
16:0	19.12 ± 0.39 [a]	16.82 ± 0.84 [b]
18:0	6.88 ± 0.21 [a]	5.98 ± 0.24 [b]
20:0	0.92 ± 0.09 [a]	0.58 ± 0.09 [b]
16:1	1.43 ± 0.08	1.37 ± 0.14
18:1	23.98 ± 0.67	20.58 ± 0.35
20:1	0.80 ± 0.06 [b]	1.02 ± 0.05 [a]
18:2n-6	33.17 ± 1.00 [a]	24.11 ± 0.75 [b]
20:3n-6	0.47 ± 0.01 [b]	2.55 ± 0.15 [a]
20:4n-6 (ARA)	0.15 ± 0.02 [b]	0.59 ± 0.03 [a]
18:3n-3	3.39 ± 0.14 [b]	15.04 ± 0.54 [a]
20:5n-3 (EPA)	0.31 ± 0.03 [b]	0.68 ± 0.04 [a]
22:6n-3 (DHA)	4.35 ± 0.22 [b]	7.34 ± 0.50 [a]
Others	5.03 ± 0.54	5.42 ± 0.43
SFA	30.51 ± 0.64 [a]	26.98 ± 1.09 [b]
MUFA	26.87 ± 0.79	23.14 ± 0.78
n-6 PUFA	34.57 ± 0.75 [a]	26.17 ± 0.83 [b]
n-3 PUFA	8.05 ± 0.28 [b]	23.71 ± 0.34 [a]
LC-PUFA	5.72 ± 0.82 [b]	11.25 ± 1.16 [a]

Note: Results are presented as the mean ± SEM (n = 4). Moisture content is expressed on a wet-weight basis, whereas crude protein and crude lipid contents are expressed on a dry-matter basis. Individual fatty acids are expressed as percentages of total identified fatty acids. SFA: 14:0, 16:0, 18:0, 20:0, 21:0, 22:0, 24:0. MUFA: 16:1, 18:1, 20:1, 22:1, 24:1. n-6 PUFA: 18:2n-6, 20:2n-6, 20:3n-6, 20:4n-6, 22:4n-6, 22:5n-6. n-3 PUFA: 18:3n-3, 20:4n-3, 20:5n-3, 22:5n-3, 22:6n-3. LC-PUFA: PUFAs with ≥20 carbons and ≥ 3 double bonds (20:3n-6, 20:4n-6, 20:5n-3, 22:5n-3, 22:6n-3). Each minor fatty acid is assigned to one of the four classes, so the four class subtotals sum to 100.00% of total fatty acids and

already include the fatty acids that are not listed individually (14:0, 21:0, 22:0, 24:0, 22:1, 24:1, 20:3n-3 and 22:5n-3). Others give the total of these non-listed fatty acids (100.00 minus the sum of the individually listed fatty acids) and are therefore not additive to the four class subtotals. Values in each row without sharing a common letter are significantly different ($p < 0.05$).

As shown in Table 3, cooking loss, water loss, and adhesiveness did not demonstrate any statistical differences between the two dietary groups ($p > 0.05$). The D2 group, however, exhibited significantly higher values for other muscle texture parameters, namely chewiness, hardness, gumminess, springiness, resilience and cohesiveness, compared with the D1 group ($p < 0.05$). These findings indicate that incorporating high ALA diets can positively impact the muscle texture of farmed tilapia.

Table 3. Edible quality and textural parameters in the muscle of tilapia fed the two different diets.

	Dietary Groups	
	D1	**D2**
Edible quality		
Cooking loss (%)	22.55 ± 1.65	22.71 ± 0.94
Water loss (%)	9.63 ± 1.58	9.28 ± 0.57
Textural parameters		
Hardness (gf)	185.11 ± 7.45 ^{b}	243.00 ± 5.40 ^{a}
Springiness	0.67 ± 0.01 ^{b}	0.70 ± 0.01 ^{a}
Chewiness (gf)	65.16 ± 3.17 ^{b}	82.97 ± 2.55 ^{a}
Gumminess (gf)	96.92 ± 4.13 ^{b}	118.65 ± 3.36 ^{a}
Cohesiveness	0.59 ± 0.01 ^{b}	0.66 ± 0.01 ^{a}
Resilience	0.36 ± 0.01 ^{b}	0.42 ± 0.01 ^{a}
Adhesiveness (gf-mm)	−0.13 ± 0.13	−0.07 ± 0.12

Results are presented as the mean ± SEM ($n = 4$). Values in each row without sharing a common letter are significantly different ($p < 0.05$).

3.3. Muscular Morphology

The histological characteristics of the muscle of tilapia were shown in Figure 1. The D2 group exhibited a significantly higher muscle fiber density compared to the D1 group ($p < 0.05$). Specifically, the percentage of small-diameter fibers (<20 μm) and medium-diameter fibers (20–50 μm) in the group of D2 was significantly higher than in the D1 group ($p < 0.05$). In turn, a high percentage of large-diameter fibers (>50 μm) were observed in the D1 group ($p < 0.05$).

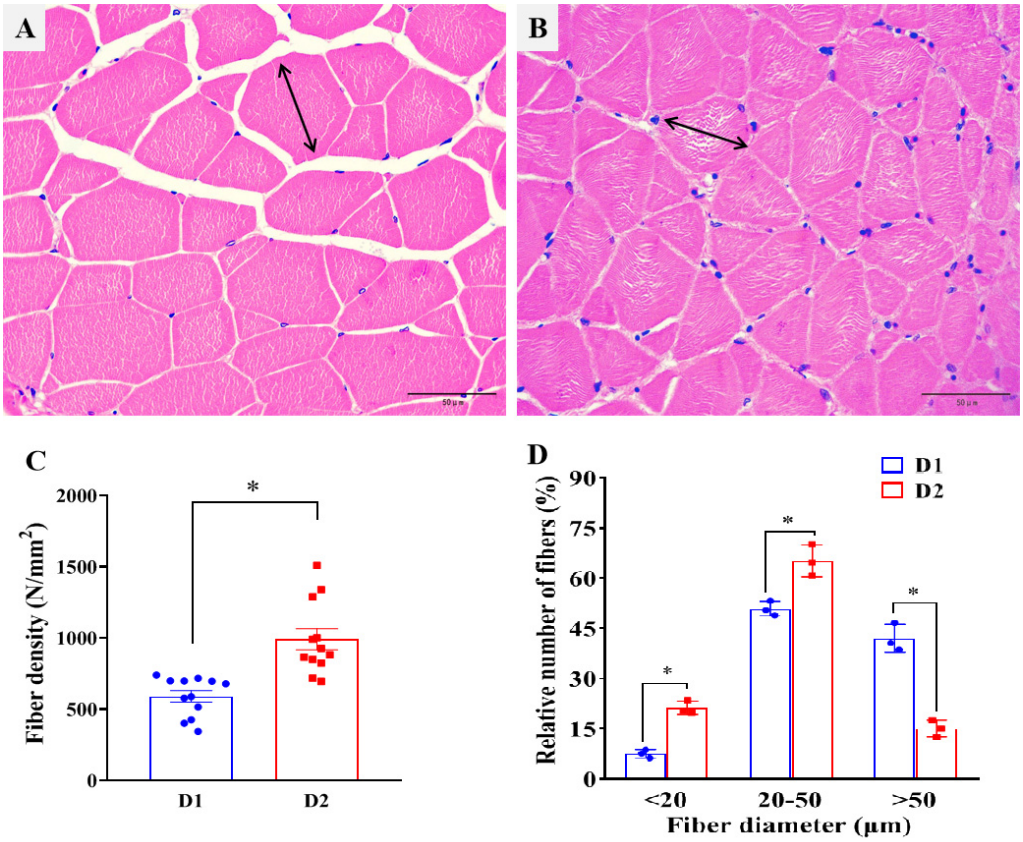


Figure 1. Histological characteristics of white muscle in tilapia fed the experimental diets ($n = 4$ cages per diet). Three fish per cage were measured and averaged, so each plotted value represents one cage. Photomicrographs of transversal sections of white muscle from tilapia fed the D1 (**A**) and D2 (**B**) diets (×400; scale bar = 50 μm). Muscle fibers (thick arrowhead) exhibit irregular polygons and are separated by the endomysium. (**C**) Muscle fiber density (N/mm²). (**D**) Muscle fiber diameter distribution. Statistical significance is denoted with asterisks as follows: * $p < 0.05$.

3.4. Transcriptome Analysis

Differential expression analysis identified 207 DEGs between D1 and D2 using DESeq2 on RSEM-derived gene-level expression values, of which 24 were up-regulated and 183 down-regulated, indicating that the transcriptional difference between the two groups is dominated by gene repression (Figure S1). GO enrichment of the DEGs (top 15 terms) was concentrated in lipid and acyl-thioester metabolism, nucleoside bisphosphate and sulfur-compound metabolism, carbohydrate and energy metabolism, and Ca^{2+}-binding/contractile components (troponin complex; highest rich factor) (Figure 2A). KEGG enrichment identified cardiac muscle contraction and adrenergic signaling in cardiomyocytes as the most prominently enriched pathways, together with lipid metabolism (primary bile acid biosynthesis, biosynthesis of unsaturated fatty acids, peroxisome, fatty acid elongation), energy metabolism (TCA cycle, fructose and mannose metabolism, nicotinate and nicotinamide metabolism), the Foxo signaling pathway, and DNA repair/nucleocytoplasmic transport (Figure 2B).

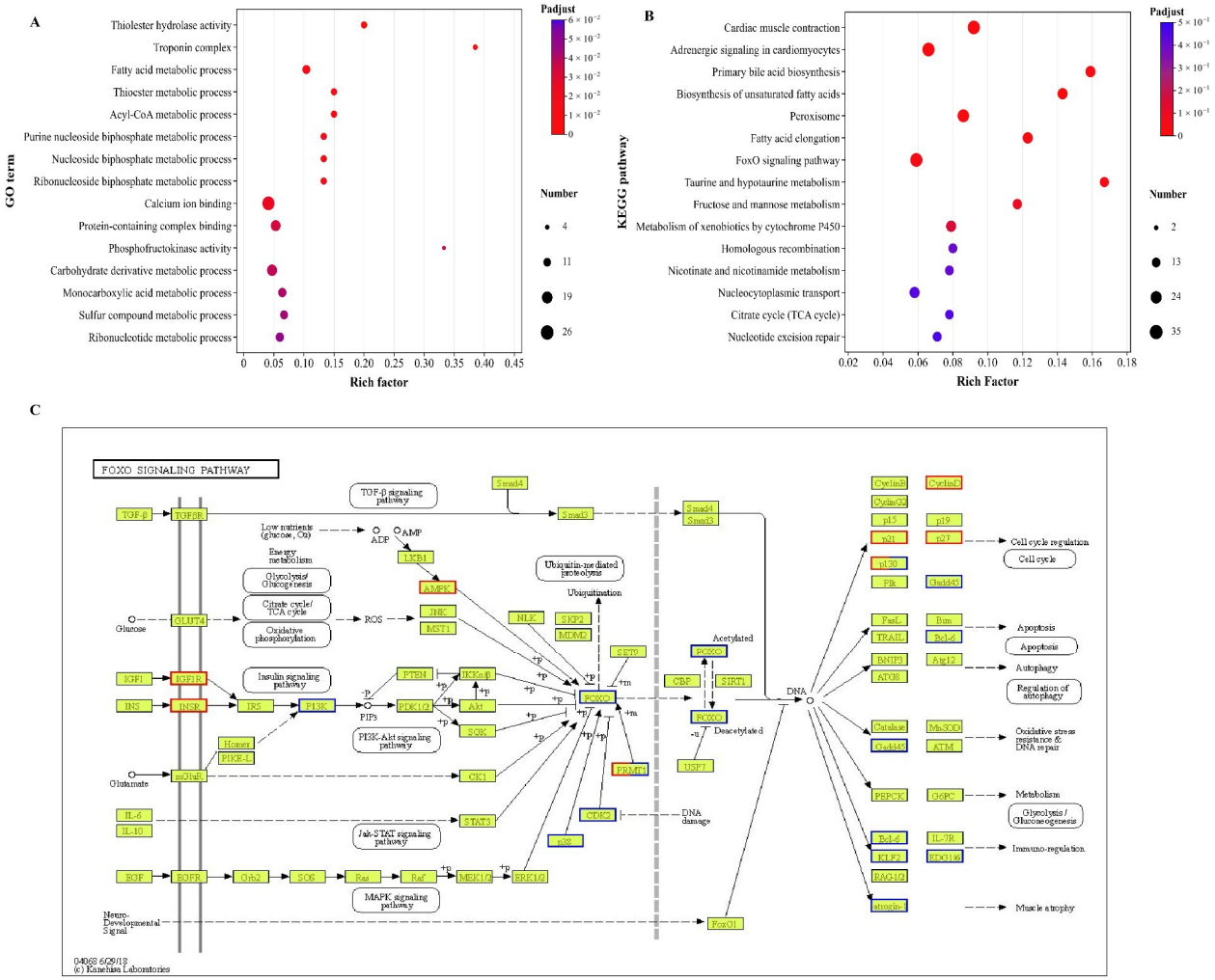


Figure 2. Functional enrichment analysis of DEGs. (**A**) Top 15 enriched Gene Ontology (GO) terms. (**B**) Top 15 enriched KEGG pathways. In (**A**) and (**B**), bubble size represents the number of DEGs annotated to the term or pathway and bubble colour represents the adjusted *p* value; the enrichment factor is defined as the ratio of DEGs to all annotated genes in a given term/pathway. (**C**) DEGs mapped onto the KEGG FOXO signaling pathway; red and blue boxes denote up- and down-regulated genes, respectively.

Mapping the DEGs onto the KEGG FoxO pathway showed that the majority of highlighted nodes were down-regulated, including the FoxO downstream effector branches (Figure 2C). Among the upstream inputs of FoxO, only the p38 Mapk-FoxO branch gave consistent results: the p38 Mapk cascade converging on Foxo, together with the JNK module, was down-regulated, and, because p38 Mapk acts upstream of Foxo and promotes its activity [18], this is expected to attenuate Foxo-dependent transcription. By contrast, the Pi3k-Akt–FoxO and Ampk-FoxO modules both contained DEGs but were regulated in the opposite direction to prediction (Pi3k-Akt being a negative and Ampk a positive regulator of FoxO), and both act post-translationally, so their mRNA levels cannot serve as proxies of FoxO activity. Collectively, the results indicate that the two groups differ mainly in contractile function, adrenergic responsiveness and energy metabolism, and suggest that the p38 Mapk-FoxO pathway may be an important pathway in the transcriptional difference between the two groups.

3.5. Correlation Analysis of Selected Genes Identifies Candidate Regulators

To prioritize candidate regulators for further validation, a gene–gene Pearson correlation matrix was constructed using 27 selected genes across six samples (three biological

replicates per dietary group, Table S4). These genes were selected based on their potential involvement in muscle development, myogenic regulation, and related signaling processes, and not all met the predefined criteria for differential expression (Figure 3). Genes were ordered by hierarchical clustering using average linkage based on a distance metric of $1 - r$, followed by optimal leaf ordering. Correlation coefficients with $|r| > 0.70$ were annotated in the corresponding cells, and the five genes with the highest mean $|r|$ were highlighted in red (Figure S2). Hierarchical clustering identified two mutually exclusive co-expression modules comprising 18 of the 27 selected genes, whereas the remaining nine (*myod*, *egf*, *egfr*, *myf4*, *pnpla8*, *myog*, *mek2*, *mek4* and *erk1*) did not form a coherent module. Module I comprised eleven genes induced in D2—*troponin C*, *troponin T*, *troponin I*, *myhc*, *myl4*, *myo7*, *stimate*, *serca1*, *serca2*, *foxo3* and *myf5*—and was highly coherent (mean intra-modular $r = 0.87$, range 0.60–1.00; 55 pairs); nine members showed higher transcript abundance in D2 ($\log_2$FC from −1.23 to −4.48, with negative values denoting higher expression in D2), whereas *foxo3* ($\log_2$FC = −0.45) and *myf5* ($\log_2$FC = 0.19) exhibited relatively small changes. The six sarcomeric genes (*troponin C, troponin T, troponin I, myhc, myl4 and myo7*) formed a strongly correlated sub-block (mean $r = 0.91$, range 0.70–0.99). Particularly strong associations were observed between *troponin I* and *troponin T* ($r = 0.958$), *Myhc* and *troponin I* (0.956), *stimate* and *troponin T* (0.955), *troponin C* and *troponin T* (0.954), *myo7* and *myl4* (0.952). The two *serca* paralogues were also highly correlated ($r = 1.000$). These findings suggest that these genes are co-regulated as a single myogenic differentiation program. Module II comprised seven genes of the D1 group, namely *mstn, foxo1, p38 mapk, mkk4, map3k, erk2* and *mek1*. This module exhibited moderate overall internal correlations (mean intra-modular $r = 0.57$, range from 0.39 to 0.93; 21 gene pairs). Five of these showed markedly lower transcript abundance in D2 on the TPM scale, whereas *erk2* and *mek1* showed relatively small differences between treatments. However, DESeq2 analysis indicated that only *foxo1* was significantly differentially expressed among these seven genes ($\log_2$FC = 1.62, padj = 0.010), whereas the remaining six genes did not reach statistical significance (padj ≥ 0.36). The four genes *mstn*, *foxo1*, *p38 mapk* and *mkk4*, which are related to atrophy and stress, exhibited relatively strong positive correlations (mean $r = 0.84$, range from 0.66 to 0.93), including *mstn-foxo1* ($r = 0.932$), *foxo1-p38 mapk* ($r = 0.921$), and *p38 mapk-mkk4* ($r = 0.916$). The two modules exhibited predominantly negative inter-module correlations (mean $r = -0.69$, ranging from −0.98 to −0.29; 77 gene pairs). For example, *mstn* was negatively correlated with *troponin T* ($r = -0.845$), whereas *foxo1* showed strong negative correlations with the six sarcomeric genes in Module I (mean $r = -0.94$, range from −0.98 to − 0.81). These findings indicate that the two groups of genes exhibited opposing expression patterns across the six samples. However, since the analysis included only three biological replicates per dietary treatment, these correlations should be interpreted as exploratory associations rather than evidence of direct regulatory interactions.

Hub analysis based on the mean absolute correlation identified *foxo1* (mean $|r| = 0.75$), *troponin T* (0.75), *myf5* (0.74), *stimate* (0.74) and *myl4* (0.74) as the most highly connected genes (the five highlighted in red in Figure S2), followed by *troponin C* (0.73), *troponin I* (0.72), *p38 mapk* (0.71), *myo7* (0.70), *mstn* (0.68), *myod* (0.68) and *mkk4* (0.68). Approximately 28.5% of the 351 gene pairs exceeded $|r| = 0.811$, corresponding to a nominal two-tailed $p < 0.05$ (df = 4). In addition, approximately 10% and 5% of the gene pairs showed correlations $r > 0.90$ and $r < -0.90$, respectively. The network therefore was dominated by a limited set of genes: *foxo1* and *p38 mapk* were the most strongly connected members of the D1-associated branch, whereas *troponin T*, *myl4*, *myf5* and *stimate* were the most strongly connected members of the D2-associated branch. Among the top five hubs, *foxo1* (padj = 0.010), *troponin T* (padj = 3.2×10^{-23}) and *myl4* (padj = 1.1×10^{-8}) reached the DESeq2 significance threshold of padj < 0.05, whereas *stimate* (padj = 0.072) and *myf5* (padj = 0.995) did not. Similarly, *p38 mapk* (padj = 0.852) and *mkk4* (padj = 0.992), which ranked eighth

and twelfth by mean $|r|$, were likewise not significant; for *p38 mapk*, although qPCR detected a difference in *p38 mapk* expression between dietary treatments (Section 3.6), this result does not change its nonsignificant status in the transcript analysis. The possible reasons for this discrepancy are discussed in Section 4.

Overall, the correlation analysis identified exploratory co-expression patterns involving genes associated with sarcomeric organization, myogenic regulation, and stress-related signaling. Considering both its network connectivity and significant differential expression, *foxo1* was prioritized as a candidate gene for further qPCR validation. Nevertheless, these findings do not establish a causal regulatory relationship between *foxo1*, *p38 mapk*, and the observed muscle phenotypes.

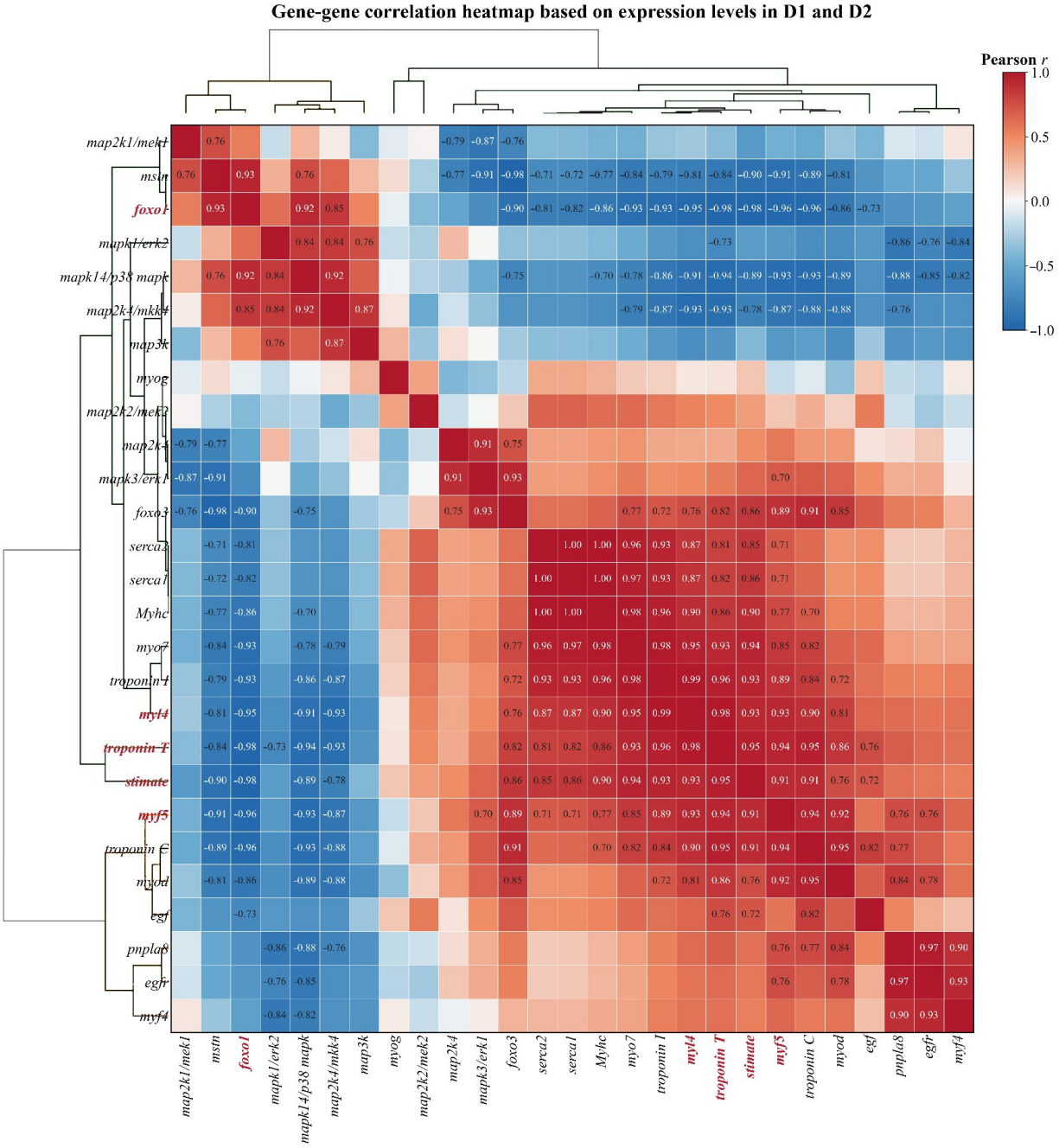


Figure 3. Gene–gene correlation heatmap of the 27 selected genes across the D1 and D2 groups. Pearson correlation coefficients were calculated for every gene pair; cells with $|r| > 0.70$ are annotated, and the five genes with the highest mean ranked by mean $|r|$ are labeled in red. Red and blue indicate positive and negative correlations, respectively.

3.6. Gene Expression in the Muscle

The relative mRNA expression of genes related to muscle myofiber development of fish fed diets D1 and D2 was shown in Figure 4. The D2 group exhibited markedly elevated mRNA expression levels of muscle *myod* and *myf5*, along with significantly decreased expression levels of *mstn* ($p < 0.05$) compared to the D1 group (Figure 4A). While the expression levels of *myf4* and *myog* mRNA were similar between the two groups ($p > 0.05$) (Figure 4A), a significant difference was observed in the expression levels of *p38 mapk* and *foxo1* between the two groups. Specifically, the D2 group exhibited decreased mRNA expression levels of *p38 mapk* and *foxo1* compared to the D1 group ($p < 0.05$) (Figure 4B).

To quantitatively evaluate the consistency between RNA-seq and qPCR data, the $\log_2$ fold-change ($\log_2$FC) values of seven genes (*foxo1*, *p38 mapk*, *mstn*, *myod*, *myf5*, *myf4*, and *myog*) obtained from both methods were subjected to Pearson correlation analysis, with RNA-seq $\log_2$FC calculated as $\log_2$(mean TPM in D2/mean TPM in D1). The DESeq2 $\log_2$FC values in Table S4 are expressed as $\log_2$(D1/D2) and are therefore of opposite sign. The results revealed a strong and significant positive correlation between the two datasets ($r = 0.885$, $p = 0.0081$; Figure S3). Furthermore, the three genes with the largest fold changes (*foxo1*, *p38 mapk* and *mstn*) showed the same direction of change in both methods, whereas the myogenic regulatory factors changed little at the transcript level ($|\log_2 FC| < 1$). This quantitative agreement supports the reliability of the transcriptomic measurements.

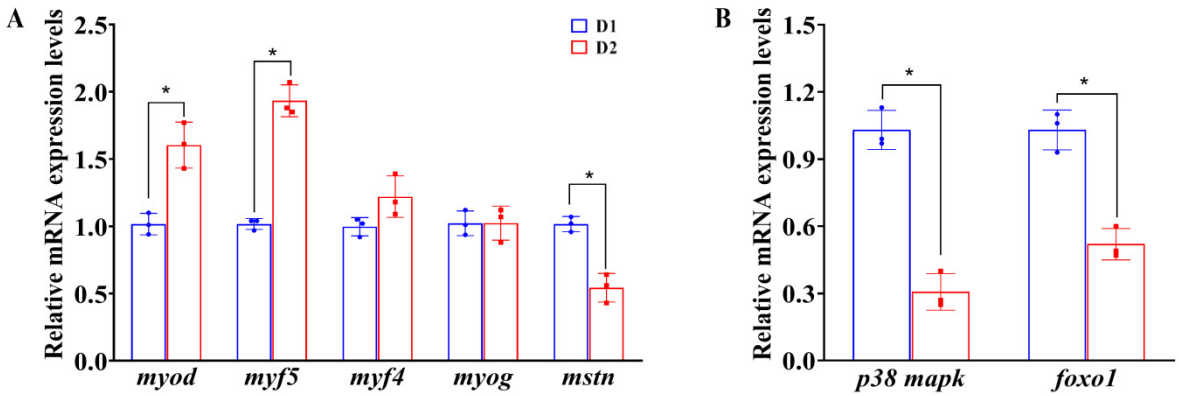


Figure 4. mRNA expression levels of genes involved in muscle development in tilapia subjected to different dietary treatments. (A) Relative mRNA expression levels of muscle development-related genes (*myod, myf5, myf4, myog, and mstn*). (B) Relative mRNA expression levels of *p38 mapk* and *foxo1*. Data are expressed as mean ± SEM ($n = 4$ cages per dietary treatment). Three fish were sampled from each cage, and their measurements were averaged to obtain one biological replicate (cage). Statistical significance is denoted with an asterisk ($p < 0.05$).

3.7. Effects of ALA Incubation on Cell Viability and the Expression of Genes Related to Myofiber Development

Cell morphology and viability of the common carp myoblast line incubated with ALA are shown in Figure 5A–C (morphology) and Figure 5D (viability). Compared with the control treatment, high cell density and viability were observed in the two ALA incubation treatments ($p < 0.05$). As illustrated in Figure 5D,E, the mRNA expression levels of *myod*, *myf5*, *myf4*, and *myog* were significantly elevated following incubation with ALA (treatment with 50 μM and 100 μM ALA) compared to the control ($p < 0.05$), and the expression of *mstn*, *p38 mapk*, and *foxo1* was significantly down-regulated in the two ALA treatments ($p < 0.05$).

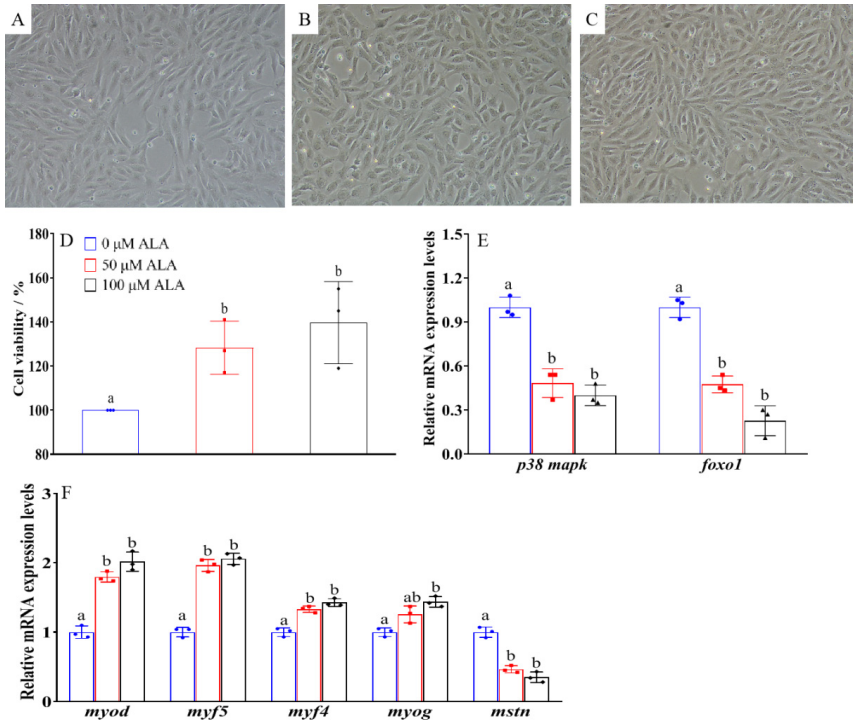


Figure 5. Morphology (**A**–**C**), cell viability (**D**), and gene (**E**,**F**) expression levels in the myoblast cell line of common carp incubated with ALA (0 μM, 50 μM, 100 μM). Data are presented as mean ± SEM (n = 3 independent experiments). Bars among each gene without sharing a common letter are significantly different among the ALA-incubated treatments ($p < 0.05$).

3.8. Effects of ALA + Hes Co-Incubation on Cell Viability and the Expression of Genes Related to Myofiber

Cell morphology (Figure 6A–D) and viability (Figure 6E) of common carp myoblasts incubated with DMSO, ALA and Hes are shown in Figure 6. Two-way ANOVA revealed a significant main effect of ALA ($p < 0.001$) and Hes ($p = 0.013$) on cell viability, but no significant interaction between them ($p = 0.813$). Specifically, compared with the control treatment, Hes treatment significantly decreased cell viability ($p < 0.05$), whereas ALA treatment significantly increased cell viability ($p < 0.05$). The ALA + Hes co-treatment group showed significantly higher viability than the Hes-alone group ($p < 0.05$), while its viability was not significantly different from that of the control group. However, the non-significant interaction indicates that these differences do not provide evidence of an ALA-specific effect of Hes on cell viability.

As depicted in Figure 7, two-way ANOVA revealed significant main effects of ALA ($p < 0.001$) and Hes ($p < 0.05$ or $p < 0.001$) on the expression of all measured genes. Specifically, compared with the DMSO control, Hes treatment significantly increased the mRNA levels of *p38 mapk*, *foxo1*, and *mstn*, while decreasing those of *myod*, *myf5*, *myf4*, and *myog* ($p < 0.05$). Conversely, ALA treatment exerted the opposite effects, significantly downregulating *p38 mapk*, *foxo1*, and *mstn*, and upregulating the myogenic factors (*myod*, *myf5*, *myf4*, and *myog*) ($p < 0.05$). The mRNA levels of all these genes in the ALA + Hes co-incubation group were comparable to those of the DMSO control group. Although this pattern suggests a potential antagonistic interaction, Hes alone also affected cell fitness, and the interaction term for cell viability was not statistically significant. Therefore, these findings do not provide sufficient evidence for a pathway-specific reversal of the effects of ALA.

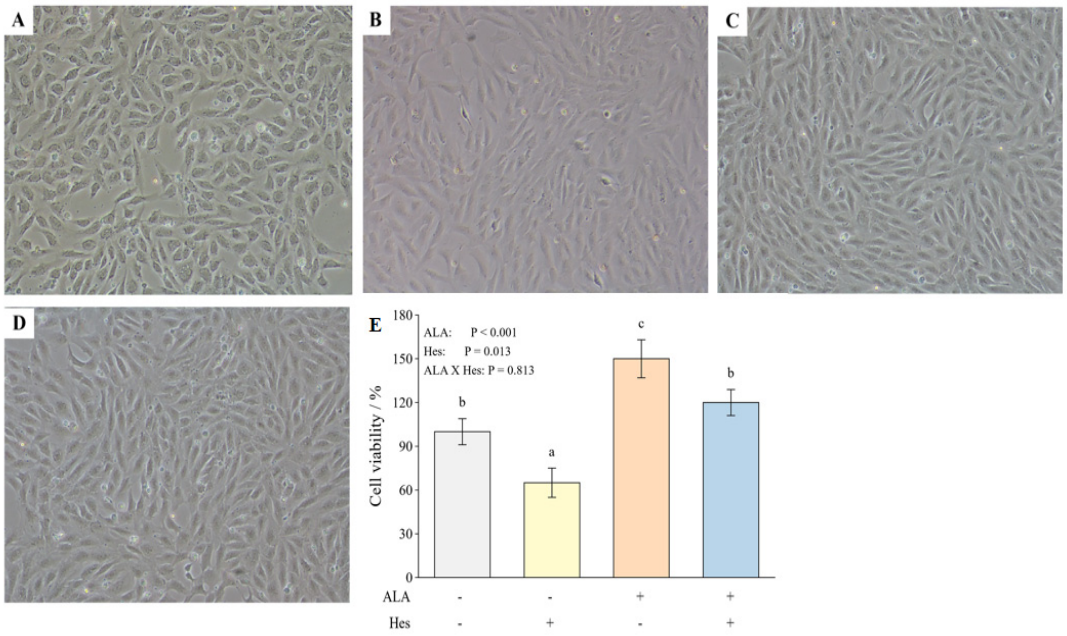


Figure 6. Morphology (**A–D**) and cell viability (**E**) of the myoblast cell line of common carp incubated with DMSO, ALA (50 μM) and Hes (400 μM). Data are presented as mean ± SEM (n = 3 independent experiments) of three replicates. Different lowercase letters above the bars indicate significant differences among groups.

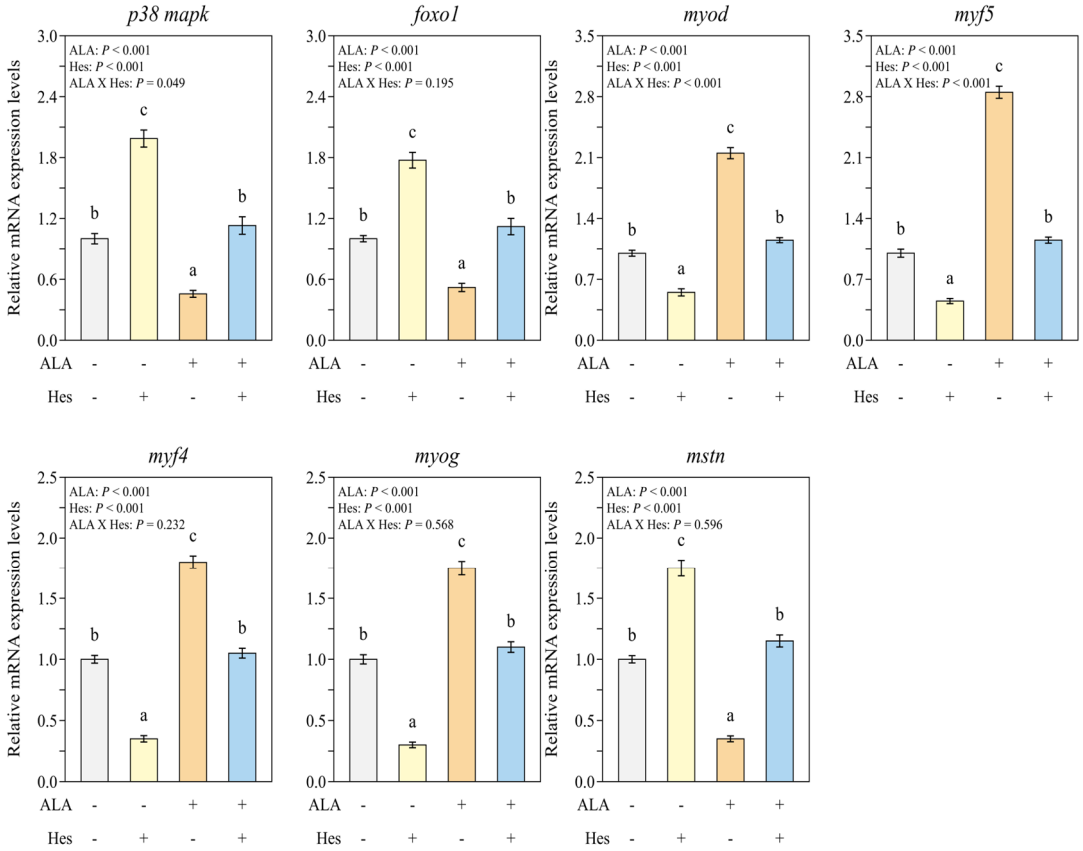


Figure 7. mRNA expression levels of genes related to muscle growth and development in the common carp myoblast cell line incubated with DMSO, ALA (50 μM) and Hes (400 μM). Data are the mean ± SEM of three replicates. Data are presented as mean ± SEM (*n* = 3 independent experiments).

Different lowercase letters above the bars indicate significant differences among treatments (Tukey's multiple-comparison test, $p < 0.05$).

4. Discussion

Nile Tilapia possess enzymatic pathways capable of converting dietary ALA into LC-PUFA, although the efficiency of this conversion depends on dietary composition and physiological conditions [7,27,33]. In the present study, growth performance, feed efficiency, and most somatic indices were statistically indistinguishable between fish fed the D2 and D1 diets, apart from a modest but significant increase in condition factor in the D2 group, which is consistent with earlier reports that dietary ALA level does not constrain growth in tilapia once essential fatty acid requirements are met [22,34]. In contrast, muscle fatty acid composition responded markedly between treatments: n-3 PUFA and total LC-PUFA increased, with a 1.97-fold increase in total LC-PUFA, whereas n-6 PUFA and SFA decreased by 24.3% and 11.6%, respectively. These differences suggest that the D2 formulation may produce a more favorable fillet fatty acid profile [35–37]. The diets differed not only in ALA content but also in oil source and several other fatty acids. Thus, the in vivo differences should be attributed to the dietary lipid formulations as a whole rather than to ALA alone.

Firm flesh is generally considered an important quality attribute in fish, making fillet texture a relevant trait for both processors and consumers [2]. In the present study, six of the seven measured textural attributes, including chewiness, hardness, gumminess, springiness, resilience and cohesiveness, were significantly higher in the D2 group, whereas adhesiveness did not differ significantly. In contrast, cooking loss, water loss, and muscle proximate composition did not differ significantly between the dietary groups. These results suggest that the dietary treatments were associated with changes in muscle mechanical properties without detectable differences in the measured water-loss parameters or muscle composition. Muscle texture is a complex trait influenced by multiple structural and biochemical factors. Cooking loss and water loss provide only partial information about muscle water retention, while other factors, including muscle pH, drip loss, collagen content and cross-linking, extracellular matrix organization, fiber-type composition, post-mortem rigor and handling effects, were not comprehensively assessed [2,38–40]. Furthermore, changes in fatty acid composition, despite similar total muscle lipid content, may also contribute to differences in texture. Therefore, the observed textural changes may reflect the combined effects of structural and biochemical factors rather than a single underlying mechanism. As sensory evaluation was not conducted, whether differences in the observed texture are perceptible or preferred by consumers remains to be determined.

Changes in muscle fiber morphology may represent one plausible contributor to the greater firmness observed in the D2 group, as the D2 group exhibited a smaller mean fiber diameter and a higher proportion of small-diameter fibers (<20 μm). While muscle fiber size and density are associated with the mechanical properties of fish muscle [2,20,21,41], texture is a complex trait also influenced by collagen content, cross-linking, and extracellular matrix organization, which were not directly measured in this study. Moreover, because morphology was evaluated at a single endpoint without direct markers of proliferation, a higher density of small fibers cannot definitively distinguish between increased hyperplasia and reduced hypertrophic growth. Therefore, the altered fiber-size distribution is presented as a plausible contributor to the texture differences rather than an established cause, and further studies integrating these structural determinants are needed.

To explore molecular processes associated with these findings, transcriptomic analysis identified *foxo1* as a highly connected gene in a co-expression module more strongly expressed in the D1 group, although only nine of the 27 genes surveyed (*foxo1*, *myosin-7*,

myosin heavy chain, *myosin light chain 4*, *troponin I*, *troponin T*, *troponin C*, *serca1* and *serca2*) reached the DESeq2 significance threshold of padj < 0.05. Myogenic regulatory factors, including *myod*, *myf5*, *myog* and *mrf4*, together with the growth inhibitor *mstn*, play important roles in regulating muscle development [14]. Previous studies have shown that dietary hydroxyproline and methionine increased the expression of *myod*, *myog* and *mrf4*, and the proportion of small-diameter fibers in Yellow River carp [42,43], whereas DHA promotes fiber development in blunt snout bream and common carp, potentially involving Ampk/Sirt1- and FoxO1-related signaling, respectively [20,21]. Consistent with these observations, D2-fed tilapia showed higher muscle *myod* and *myf5* transcripts, and lower *mstn* expression, whereas *myf4* and *myog* remained unchanged. In contrast, incubation with ALA up-regulated the expression of *myf4*, *myf5*, *myog* and *myod* in cultured common carp myoblasts. These differences in gene expression may reflect variations in cellular composition, differentiation state, exposure duration, or species-specific responses. Therefore, the in vitro findings should be regarded as supporting cross-species evidence rather than direct validation of the myogenic responses in Nile tilapia. Moreover, since the two experimental diets differed in lipid source and overall fatty acid composition rather than solely in ALA content, the observed in vivo changes cannot be attributed exclusively to ALA. Although the cell-based experiments using purified ALA provide additional evidence of its cellular effects, they do not resolve the potential confounding effects of the different lipid formulations. Though these findings are consistent with altered myogenic regulation, changes in gene expression and cell viability do not directly establish enhanced myoblast proliferation or new muscle fiber recruitment in Nile tilapia. The higher proportion of small-diameter fibers may also reflect slower hypertrophy of existing fibers. Recent work has highlighted the involvement of fatty acid uptake and downstream signaling in myogenic regulation [44,45], providing additional biological context for the present findings without establishing a specific causal signaling mechanism.

FoxO1 participates in the regulation of myogenic programs [16,46–50], and p38 Mapk signaling has been implicated in myogenic and stress-related responses in muscle cells [51–54], direct crosstalk between the two has been reported in non-muscle mammalian cells, where p38 phosphorylates and regulates FoxO1 [18]. In the present study, *foxo1* transcript abundance was lower in the muscle of D2-fed tilapia. In common carp myoblasts, purified ALA was associated with reduced abundance of the assayed p38 mapk-related transcript and of *foxo1*, accompanied by increased cell density and viability. Hesperetin co-treatment attenuated these ALA-associated responses, but hesperetin alone also reduced cell viability, indicating that the attenuation more likely reflects a general effect on cell fitness than selective interference with p38 Mapk. This interpretation is consistent with hesperetin not being a selective p38 Mapk modulator: it has been reported to activate p38 in glioblastoma and venous smooth muscle cells, to suppress it in microglia, chondrocytes and PRRSV-infected cells, and to leave p38 phosphorylation unchanged in C_2C_{12} myotubes [55–60]. Its effects therefore cannot be taken as evidence of a specific p38 Mapk-FoxO1 signaling sequence. Because p38 Mapk acts at more than one stage of myogenesis and its effects differ between isoforms p38α promoting cell-cycle exit and differentiation, whereas p38γ supports the expansion of myogenic precursors by preventing premature differentiation [19], the co-occurrence of lower *p38 mapk* transcript abundance with higher myoblast density is interpreted as a shift towards maintained proliferation and delayed differentiation, rather than as p38 Mapk being dispensable for myogenesis. Two further limitations should be acknowledged. First, p38 Mapk activity is primarily regulated by phosphorylation, whereas FoxO1 function is influenced by phosphorylation and subcellular localization. However, neither the phosphorylated-to-total ratios nor FoxO1 nuclear localization were assessed in the present study. Second, no pathway-specific genetic perturbation experiments were conducted to establish a causal relationship. Moreover, the

observed changes in myoblast viability and myogenic gene expression may reflect maintained cell proliferation, delayed myogenic differentiation, or broader effects of Hes on cellular fitness. Accordingly, the present findings indicate an association between ALA-related cellular responses and p38 Mapk/FoxO1-related transcriptional changes, but do not establish altered pathway activity, the order of signaling events, or a causal role for this pathway in mediating the effects of ALA.

Several limitations should be considered. First, the two lipid formulations differed in multiple fatty acids in addition to ALA, and only two ALA levels were compared; the optimal dietary level and the response to levels above 35.78% of total fatty acids therefore remain undetermined. Second, the purified-ALA experiments provide supportive mechanistic context but do not eliminate this dietary confounding, and the use of common carp myoblasts may limit extrapolation to Nile tilapia because of species-specific differences. Third, muscle histology was assessed at a single endpoint, without direct measurement of myoblast proliferation, fiber recruitment or collagen properties. Fourth, as noted above, the p38 Mapk/FoxO1 inference rests on transcript abundance alone, without phosphorylation, localization or genetic-perturbation readouts. Addressing these gaps will require tightly controlled lipid formulations spanning multiple ALA levels, tilapia-derived myogenic cells, direct assessment of fiber and collagen organization, and genetic manipulation of the pathway combined with protein-level and localization analyses. Fifth, of the 27 genes examined by RNA-seq, only nine were significant at padj < 0.05 after Benjamini–Hochberg correction, eight of which encode sarcomeric or calcium-handling proteins and one of which (*foxo1*) encodes a transcription factor; the *p38 mapk*, *map2k4* (*mkk4*) and *foxo3* transcripts included in the panel did not reach this threshold (padj = 0.852, 0.992 and 0.844, respectively), so the transcriptional differences reported here should be read as hypothesis-generating rather than as evidence of differential pathway activity. Two considerations explain why the *p38 mapk* transcript did not reach this threshold although qPCR detected a significant decrease in the D2 group, and the two results should not be read as contradictory. First, the effect size is modest: $\log_2$FC = 0.76, corresponding to a 1.7-fold difference, which falls below the $|\log_2 FC| \geq 1$ criterion conventionally applied to define DEGs. That criterion is readily met by the strongly induced sarcomeric and calcium-handling genes but is stringent for signaling transcripts, whose transcriptional regulation is typically moderate; because p38 Mapk activity is governed principally by phosphorylation rather than by transcript abundance, a modest transcriptional change is also consistent with the underlying biology. Second, with three replicates per group and Benjamini–Hochberg correction applied across the whole transcriptome, the DESeq2 test has limited power for effects of this size, so padj = 0.852 indicates insufficient evidence rather than demonstrated absence of a difference. The two datasets agree in direction and magnitude, and the conclusion that p38 mapk transcript abundance is lower in the D2 group therefore rests on the qPCR evidence, with the RNA-seq data providing directionally consistent support.

5. Conclusions

In conclusion, the linseed-oil-based formulation, in which ALA increased from 8.42% to 35.78% of total fatty acids, was associated with a more favorable muscle fatty acid profile and improved texture characteristics in Nile tilapia fillets. Cell-based findings indicate that p38 Mapk/FoxO1-related signaling may be involved in ALA-associated changes in myoblast activity and myogenic gene expression. However, given the differences in overall dietary fatty acid composition and the primarily transcript-level observations, this signaling pathway should be considered a candidate mechanism rather than an established causal mediator. Future studies using targeted genetic approaches are required to verify this mechanism.

Supplementary Materials: The following supporting information can be downloaded at: https://www.mdpi.com/article/10.3390/life16111916/s1, Table S1: Formulation and composition of the different experimental diets; Table S2: qPCR primer sequences used in this study. Table S3: Sequencing quality and read-mapping statistics of the six RNA-seq libraries; Table S4: Transcript expression levels of the genes screened from the GO (troponin complex), KEGG (FoxO pathway) enrichment analyses, and myogenic regulatory factors; Figure S1: DEG statistics for D1 vs. D2. Up- and down-regulated DEGs (adjusted $p < 0.05$) were identified using DESeq2; bars show the counts of up-regulated, down-regulated and total DEGs; Figure S2: Hub-gene ranking of the DEGs based on their mean absolute correlation coefficient $|r|$ with all other DEGs. Bars are coloured by branch association (blue, D1-associated; red, D2-associated), and the names of the top five hub genes are highlighted in red; Figure S3: Correlation of $\log_2$ fold-change values between RNA-seq and qPCR. The $\log_2$ fold-change ($\log_2$FC) of seven selected genes (*foxo1, p38 mapk, mstn, myod, myf5, myf4, and myog*) was calculated from both RNA-seq and qPCR data.

Author Contributions: Formal analysis, data curation, writing—original draft preparation, F.C.; resources, investigation, validation, H.Z.; data curation, Z.M.; funding acquisition, methodology, writing—review and editing, Y.L.; conceptualization, supervision, funding acquisition, project administration, writing—review and editing, D.X. All authors have read and agreed to the published version of the manuscript.

Funding: This research was funded by the grant from the Guangdong Basic and Applied Basic Research Foundation (2024A1515030246), and by the National Natural Science Foundation of China (U22A20532).

Institutional Review Board Statement: The study was conducted in accordance with the ethical guidelines for animal care and use established by South China Agricultural University. All experimental procedures were reviewed and approved by the University's Animal Ethics Committee (SYXK-2019-0136, approved on 7 June 2022).

Informed Consent Statement: Not applicable.

Data Availability Statement: The RNA-seq data generated in this study are part of an ongoing research project and are therefore not publicly available at this stage. All other data supporting the findings of this study are available from the corresponding author upon reasonable request.

Conflicts of Interest: The authors declare no conflicts of interest.

Abbreviations

The following abbreviations are used in this manuscript:

ALA	α-linolenic acid
CF	condition factor
CL	cooking loss
DEGs	differentially expressed genes
DHA	docosahexaenoic acid
FAME	Fatty acid methyl esters
FCR	feed conversion ratio
FoxO1	forkhead box O1
GC	gas chromatography
GO	Gene Ontology
HSI	hepatosomatic index
KEGG	Kyoto Encyclopedia of Genes and Genomes
LC-PUFA	long-chain polyunsaturated fatty acids
Mapk	Mitogen-Activated Protein Kinase
mstn	Myostatin
MUFA	Monounsaturated fatty acids
myf	Myogenic Factor

myod	Myogenic Differentiation
myog	Myogenin
qPCR	Quantitative real-time PCR
SE	Standard Error
SFA	Saturated Fatty Acid
SGR	specific growth rate
SUR	survival rate
TPM	transcripts per million
VSI	viscerosomatic index
WL	water loss
WGR	weight gain rate

References

1. FAO. *The State of World Fisheries and Aquaculture 2026: Sustainability in Action*; Food and Agriculture Organization of the United Nations: Rome, Italy, 2026. https://doi.org/10.4060/cd8357en.
2. Wang, Z.; Qiao, F.; Zhang, W.; Parisi, G.; Du, Z.; Zhang, M. The flesh texture of teleost fish: Characteristics and interventional strategies. *Rev. Aquac.* **2024**, *16*, 508–535. https://doi.org/10.1111/raq.12849.
3. Munguti, J.; Muthoka, M.; Mboya, J.B.; Kyule, D.; Meenakshisundaram, M.; Tanga, C.M. Unraveling the potential of black soldier fly larvae as a sustainable protein source for Nile tilapia production in diverse aquaculture systems. *Aquac. Nutr.* **2025**, *2025*, 3598843. https://doi.org/10.1155/anu/3598843.
4. Liu, W.; Li, E.; Xu, C.; Chen, L.; Wang, X. Nutritional strategies for Nile tilapia: Protein and carbohydrate balances in saline-alkaline aquaculture. *J. Anim. Sci. Biotechnol.* **2025**, *16*, 86. https://doi.org/10.1186/s40104-025-01215-8.
5. Ng, W.K.; Chong, C.; Wang, Y.; Romano, N. Effects of dietary fish and vegetable oils on the growth, tissue fatty acid composition, oxidative stability and vitamin E content of red hybrid tilapia and efficacy of using fish oil finishing diets. *Aquaculture* **2013**, *372*, 97–110. https://doi.org/10.1016/j.aquaculture.2012.10.030.
6. Wu, F.; Wen, H.; Tian, J.; Jiang, M.; Liu, W.; Yang, C. Effect of stocking density on growth performance, serum biochemical parameters, and muscle texture properties of genetically improved farm tilapia, *Oreochromis niloticus*. *Aquac. Int.* **2018**, *26*, 1247–1259. https://doi.org/10.1007/s10499-018-0281-z.
7. Xie, D.; Guan, J.; Huang, X.; Xu, C.; Pan, Q.; Li, Y. Tilapia can be a beneficial n-3 LC-PUFA source due to its high biosynthetic capacity in the liver and intestine. *J. Agric. Food Chem.* **2022**, *70*, 2701–2711. https://doi.org/10.1021/acs.jafc.1c05755.
8. Chen, F.; Lou, Y.; Guan, J.; Lan, X.; Su, Z.; Xu, C.; Li, Y.; Xie, D. Rapeseed and palm oils can improve the growth, muscle texture, fatty acids and volatiles of marine teleost golden pompano fed low fish oil diets. *Foods* **2025**, *14*, 788. https://doi.org/10.3390/foods14050788.
9. Pasomboon, P.; Kumkhong, S.; Panserat, S.; Boonanuntanasarn, S. Linseed oil injection into the yolk reserve strongly modulates lipid gene expression and fatty acid composition in juvenile Nile tilapia. *Animal* **2025**, *19*, 101647. https://doi.org/10.1016/j.animal.2025.101647.
10. Zeng, X.; Zhou, X.; Jiang, W.; Wu, P.; Liu, Y.; Ma, Y.; Jin, X.; Ren, H.; Feng, L. Histidine improves flesh quality: An assessment of grass carp (*Ctenopharyngodon idella*) muscle in terms of texture, nutritional value and flavor. *Food Chem.* **2025**, *474*, 143214. https://doi.org/10.1016/j.foodchem.2025.143214.
11. Zhang, R.; Li, H.; Wang, X.; Liu, L.; Zhu, H. Potential benefits of glycine, proline and hydroxyproline on growth and flesh quality of mirror carp (*Cyprinus carpio* var. specularis). *Int. J. Mol. Sci.* **2025**, *26*, 9011. https://doi.org/10.3390/ijms26189011.
12. Yadata, G.W.; Guo, N.X.; Meng, Z.C.; Zhao, Y.; Zhao, J. Faba bean (*Vicia faba* L.) in aquafeeds: Impacts on fish muscle quality, molecular mechanisms, and crispness attributes. *Fish Physiol. Biochem.* **2026**, *52*, 68. https://doi.org/10.1007/s10695-026-01687-z.
13. Peng, L.; You, J.; Liu, R.; Long, Y.; Song, G.; Benjakul, S.; Xiong, S.; Rahman, Z.; Huang, Q.; Chen, S.; et al. Fasting influences the muscle quality of fish during transportation by regulating the balance between energy metabolism and ammonia nitrogen stress. *J. Adv. Res.* **2026**, *79*, 75–88. https://doi.org/10.1016/j.jare.2025.03.047.
14. Koganti, P.; Yao, J.; Cleveland, B.M. Molecular mechanisms regulating muscle plasticity in fish. *Animals* **2021**, *11*, 61. https://doi.org/10.3390/ani11010061.
15. Joshi, A.S.; Tomaz da Silva, M.; Kumar, S.; Kumar, A. Signaling networks governing skeletal muscle growth, atrophy, and cachexia. *Skelet. Muscle* **2025**, *15*, 29. https://doi.org/10.1186/s13395-025-00397-z.
16. Xu, M.; Chen, X.; Chen, D.; Yu, B.; Huang, Z. FoxO1: A novel insight into its molecular mechanisms in the regulation of skeletal muscle differentiation and fiber type specification. *Oncotarget* **2017**, *8*, 10662–10674. https://doi.org/10.18632/oncotarget.12891.

17. Oyabu, M.; Sakaue, M.; Kubo, A.; Yoshioka, K.; Kawaguchi, R.; Yamamoto, H.; Kinjo, Y.; Kwon, J.; Nishi, H.; Yamanaka, D.; et al. Loss of FoxO in skeletal muscle leads to disrupted muscle metabolism and exacerbates starvation-induced hepatic steatosis. *Proc. Natl. Acad. Sci. USA* **2026**, *123*, e2600036123. https://doi.org/10.1073/pnas.2600036123.
18. Asada, S.; Daitoku, H.; Matsuzaki, H.; Saito, T.; Sudo, T.; Mukai, H.; Iwashita, S.; Kako, K.; Kishi, T.; Kasuya, Y.; et al. Mitogen-activated protein kinases, Erk and p38, phosphorylate and regulate Foxo1. *Cell. Signal.* **2007**, *19*, 519–527. https://doi.org/10.1016/j.cellsig.2006.08.015.
19. Gillespie, M.A.; Le Grand, F.; Scimè, A.; Kuang, S.; von Maltzahn, J.; Seale, V.; Cuenda, A.; Ranish, J.A.; Rudnicki, M.A. p38-γ-dependent gene silencing restricts entry into the myogenic differentiation program. *J. Cell Biol.* **2009**, *187*, 991–1005. https://doi.org/10.1083/jcb.200907037.
20. Wang, C.; Liu, W.; Huang, Y.; Wang, X.; Li, X.; Zhang, D.; Jiang, G. Dietary DHA affects muscle fiber development by activating AMPK/Sirt1 pathway in blunt snout bream (*Megalobrama amblycephala*). *Aquaculture* **2020**, *518*, 734835. https://doi.org/10.1016/j.aquaculture.2019.734835.
21. He, Z.; Xu, C.; Chen, F.; Lou, Y.; Nie, G.; Xie, D. Dietary DHA Enhanced the Textural Firmness of Common Carp (*Cyprinus carpio* L.) Fed Plant-Derived Diets through Restraining FoxO1 Pathways. *Foods* **2022**, *11*, 3600. https://doi.org/10.3390/foods11223600.
22. Huang, X.; Chen, F.; Guan, J.; Xu, C.; Li, Y.; Xie, D. Beneficial effects of re-feeding high alpha-linolenic acid diets on the muscle quality, cold temperature and disease resistance of tilapia. *Fish Shellfish Immunol.* **2022**, *126*, 303–310. https://doi.org/10.1016/j.fsi.2022.05.053.
23. Zhu, W.; Xiao, X.; Yan, Y.; Yu, C.; Fei, D.; Cao, Z.; Wan, Y.; Ommati, M.M.; Huang, Y. Comparative transcriptome analysis reveals ncRNA-mediated regulatory networks associated with muscle crispiness in grass carp. *Comp. Biochem. Physiol. D* **2026**, *60*, 101942. https://doi.org/10.1016/j.cbd.2026.101942.
24. Li, Q.; Huang, Y.; Xie, X.; Liang, S.; Lin, L. Transcriptome analysis revealed the effects of dietary faba bean (*Vicia faba* L.) on muscle quality of Nile tilapia (*Oreochromis niloticus*). *Comp. Biochem. Physiol. D* **2026**, *58*, 101747. https://doi.org/10.1016/j.cbd.2026.101747.
25. Sahoo, V.L.; Sathiyanarayanan, A.; Pinto, N.; Iqbal, G.; Yashwanth, B.; Sonwane, A.A.; Rasal, K.D.; Goswami, M. Development and proteome characterization of a new muscle cell line from *Oreochromis niloticus* (Linnaeus, 1758). *Differentiation* **2026**, *147*, 100934. https://doi.org/10.1016/j.diff.2026.100934.
26. Zheng, X.; Lin, J.; Wang, L.; Song, K.; Lu, K.; Li, X.; Zhang, C. Establishment and characterization of muscle cell line of spotted seabass (*Lateolabrax maculatus*). *Fish Physiol. Biochem.* **2025**, *51*, 161. https://doi.org/10.1007/s10695-025-01570-3.
27. You, C.; Lu, F.; Wang, S.; Chen, C.; Li, Y. Comparison of the growth performance and long-chain PUFA biosynthetic ability of the genetically improved farmed tilapia (*Oreochromis niloticus*) reared in different salinities. *Br. J. Nutr.* **2019**, *121*, 374–383. https://doi.org/10.1017/S0007114518003471.
28. Li, Y.; Monroig, Ó.; Zhang, L.; Wang, S.; Zheng, X.; Dick, J.R.; You, C.; Tocher, D.R. Vertebrate fatty acyl desaturase with Δ4 activity. *Proc. Natl. Acad. Sci. USA* **2010**, *107*, 16840–16845. https://doi.org/10.1073/pnas.1008429107.
29. Ma, Y.; Li, M.; Xie, D.; Chen, S.; Dong, Y.; Wang, M.; Zhang, G.; Zhang, M.; Chen, H.; Ye, R.; et al. Fishmeal can be replaced with a high proportion of terrestrial protein in the diet of the carnivorous marine teleost (*Trachinotus ovatus*). *Aquaculture* **2020**, *519*, 734910. https://doi.org/10.1016/j.aquaculture.2019.734910.
30. Valente, L.M.P.; Cabral, E.M.; Sousa, V.; Cunha, L.M.; Fernandes, J.M.O. Plant protein blends in diets for Senegalese sole affect skeletal muscle growth, flesh texture and the expression of related genes. *Aquaculture* **2016**, *453*, 77–85. https://doi.org/10.1016/j.aquaculture.2015.11.034.
31. Almeida, F.L.A.D.; Carvalho, R.F.; Pinhal, D.; Padovani, C.R.; Martins, C.; Dal Pai-Silva, M. Differential expression of myogenic regulatory factor MyoD in pacu skeletal muscle (*Piaractus mesopotamicus* Holmberg 1887: Serrasalminae, Characidae, Teleostei) during juvenile and adult growth phases. *Micron* **2008**, *39*, 1306–1311. https://doi.org/10.1016/j.micron.2008.02.011.
32. Zhi, S.; Wang, J.; Wang, Y.; Yang, L.; Qin, C.; Yan, X.; Zhao, M.; Liu, M.; Qu, L.; Nie, G. Establishment and characterization of Yellow River carp (*Cyprinus carpio* haematopterus) muscle cell line and its application to fish virology and immunology. *Fish Shellfish Immunol.* **2023**, *139*, 108859. https://doi.org/10.1016/j.fsi.2023.108859.
33. Xie, D.; Chen, C.; Dong, Y.; You, C.; Wang, S.; Monroig, Ó.; Tocher, D.R.; Li, Y. Regulation of long-chain polyunsaturated fatty acid biosynthesis in teleost fish. *Prog. Lipid Res.* **2021**, *82*, 101095. https://doi.org/10.1016/j.plipres.2021.101095.
34. El-Husseiny, O.M.; Abdul-Aziz, G.M.; Goda, A.; Suloma, A. Effect of altering linoleic acid and linolenic acid dietary levels and ratios on the performance and tissue fatty acid profiles of Nile tilapia *Oreochromis niloticus* fry. *Aquac. Int.* **2010**, *18*, 1105–1119. https://doi.org/10.1007/s10499-010-9327-6.

35. Chen, C.; Guan, W.; Xie, Q.; Chen, G.; He, X.; Zhang, H.; Guo, W.; Chen, F.; Tan, Y.; Pan, Q. n-3 essential fatty acids in Nile tilapia, *Oreochromis niloticus*: Bioconverting LNA to DHA is relatively efficient and the LC-PUFA biosynthetic pathway is substrate limited in juvenile fish. *Aquaculture* **2018**, *495*, 513–522. https://doi.org/10.1016/j.aquaculture.2018.06.023.
36. Li, H.; Liu, X.; Yang, F.; He, D.; Wang, P.; Wu, K. Dietary cinnamon essential oil improves the amino acids, lipid quality, long-chain polyunsaturated fatty acid biosynthesis, and gut microbiota of Nile tilapia. *J. Sci. Food Agric.* **2026**, *online ahead of print*. https://doi.org/10.1002/jsfa.70935.
37. Perez-Velazquez, M.; Encinas-Mungarro, J.; González-Félix, M.L. Rate of change in the fillet fatty acid profile of Nile tilapia to attain a nutraceutical level of DHA+ EPA for human consumption. *Aquaculture* **2024**, *580*, 740270. https://doi.org/10.1016/j.aquaculture.2023.740270.
38. Fu, B.; Xie, J.; Kaneko, G.; Wang, G.; Yang, H.; Tian, J.; Xia, Y.; Li, Z.; Gong, W.; Zhang, K.; et al. MicroRNA-dependent regulation of targeted mRNAs for improved muscle texture in crisp grass carp fed with broad bean. *Food Res. Int.* **2022**, *155*, 111071. https://doi.org/10.1016/j.foodres.2022.111071.
39. Li, Y.; Zhang, J.; Fu, B.; Xie, J.; Wang, G.; Tian, J.; Xia, Y.; Yu, E. Textural quality, growth parameters and oxidative responses in Nile tilapia (*Oreochromis niloticus*) fed faba bean water extract diet. *PeerJ* **2022**, *10*, e13048. https://doi.org/10.7717/peerj.13048.
40. Song, D.; Yun, Y.; He, Z.; Mi, J.; Luo, J.; Jin, M.; Zhou, Q.; Nie, G. Effects of faba bean (*Vicia faba* L.) on fillet quality of Yellow River carp (*Cyprinus carpio*) via the oxidative stress response. *Food Chem.* **2022**, *388*, 132953. https://doi.org/10.1016/j.foodchem.2022.132953.
41. Huang, F.; Zhan, Z.; Luo, J.; Liu, Z.; Peng, J. Duration of dietary linseed feeding affects the intramuscular fat, muscle mass and fatty acid composition in pig muscle. *Livest. Sci.* **2008**, *118*, 132–139. https://doi.org/10.1016/j.livsci.2008.01.002.
42. Song, D.; Yun, Y.; He, Z.; Mi, J.; Wang, L.; Jin, M.; Zhou, Q.; Nie, G. Fillet texture, physicochemical indexes, muscle cellularity and molecular expression in muscle of Yellow River carp (*Cyprinus carpio* haematopterus) in response to dietary hydroxyproline supplementation. *Aquaculture* **2022**, *549*, 737783. https://doi.org/10.1016/j.aquaculture.2021.737783.
43. Yun, Y.; Song, D.; He, Z.; Mi, J.; Wang, L.; Nie, G. Effects of methionine supplementation in plant protein based diet on growth performance and fillet quality of juveniles Yellow River carp (*Cyprinus carpio* haematopterus). *Aquaculture* **2022**, *549*, 737810. https://doi.org/10.1016/j.aquaculture.2021.737810.
44. Ji, S.; Li, H.; Huang, X.; Sun, J.; Kaneko, G.; Ji, H. Docosahexaenoic acid (DHA) promotes grass carp (*Ctenopharyngodon idella)* muscle fiber development by activating MEK/ERK pathway in vitro and in vivo. *Aquaculture* **2024**, *579*, 740148. https://doi.org/10.1016/j.aquaculture.2023.740148.
45. Xue, R.; Zhou, L.; Jia, L.; Zhang, J.; Li, H.; Zhao, T.; Sun, J.; Ji, H. PPARα-CD36-CAV1-mediated docosahexaenoic acid (DHA) uptake promotes muscle fiber development in grass carp (*Ctenopharyngodon idellus*). *Anim. Nutr.* **2026**, *25*, 73–88. https://doi.org/10.1016/j.aninu.2025.10.011.
46. Ru, W.; Liu, K.; Yang, J.; Liu, J.; Qi, X.; Huang, B.; Chen, H. miR-183/96/182 cluster regulates the development of bovine myoblasts through targeting FoxO1. *Animals* **2022**, *12*, 2799. https://doi.org/10.3390/ani12202799.
47. Zhang, D.; Zhang, X.; Liu, Z.; Ma, X.; Li, H.; Shen, M.; Chen, J.; Liu, H. Diosmin Promotes Myogenesis via Activating the Akt/FOXO1 Pathway to Facilitate the Proliferation of C2C12 Myoblasts. *J. Agric. Food Chem.* **2023**, *71*, 19705–19716. https://doi.org/10.1021/acs.jafc.3c04828.
48. Jiang, C.; Zhang, J.; Song, Y.; Song, X.; Wu, H.; Jiao, R.; Li, L.; Zhang, G.; Wei, D. FOXO1 regulates bovine skeletal muscle cells differentiation by targeting MYH3. *Int. J. Biol. Macromol.* **2024**, *260*, 129643. https://doi.org/10.1016/j.ijbiomac.2024.129643.
49. Deng, K.; Su, Y.; Liu, Z.; Wu, J.; Hu, S.; Zhang, Z.; Ren, C.; Liu, Z.; Wang, L.; Fan, Y.; et al. Mettl3-mediated FOXO1 mRNA translation inhibits myoblast differentiation and fusion through the MyoD1-Myomaker/Myomixer axis and the ubiquitin-proteasome system. *Int. J. Biol. Macromol.* **2026**, *374*, 153351. https://doi.org/10.1016/j.ijbiomac.2026.153351.
50. Lei, S.; Chen, R.; Shi, H.; Zhou, S.; She, Y. lncRNA AK159072 promotes myoblast proliferation and muscle regeneration through activation of Akt/Foxo1 pathway. *J. Biochem. Mol. Toxicol.* **2025**, *39*, e70292. https://doi.org/10.1002/jbt.70292.
51. Chae, J.; Hahn, D.; Nam, J.O. Macamide, a component of maca (*Lepidium meyenii* Walp) lipophilic extract, enhances myogenic differentiation via AKT/p38 signaling and attenuates dexamethasone-induced muscle atrophy. *Biomed. Pharmacother.* **2024**, *172*, 116249. https://doi.org/10.1016/j.biopha.2024.116249.
52. Jiang, M.; Zhang, H.; Zhai, L.; Ye, B.; Cheng, Y.; Zhai, C. ALA/LA ameliorates glucose toxicity on HK-2 cells by attenuating oxidative stress and apoptosis through the ROS/p38/TGF-β 1 pathway. *Lipids Health Dis.* **2017**, *16*, 216. https://doi.org/10.1186/s12944-017-0611-6.
53. Huang, S.; Taylor, C.G.; Zahradka, P. Growth state-dependent activation of eNOS in response to DHA: Involvement of p38 MAPK. *Int. J. Mol. Sci.* **2023**, *24*, 8346. https://doi.org/10.3390/ijms24098346.

54. Yu, H.; Gong, Z.; Wang, G.; Cao, R.; Yin, H.; Ma, L.; Guo, A. DHA attenuates cartilage degeneration by mediating apoptosis and autophagy in human chondrocytes and rat models of osteoarthritis. *In Vitro Cell. Dev. Biol.-Anim.* **2023**, *59*, 455–466. https://doi.org/10.1007/s11626-023-00781-3.
55. Zhang, H.; Lin, L.; Yang, A.; Liang, Y.; Huang, B. Scutellarin alleviates tensile stress-induced proliferation and migration of venous smooth muscle cells via mediating the p38 MAPK pathway. *Tissue Cell* **2024**, *87*, 102300. https://doi.org/10.1016/j.tice.2024.102300.
56. Li, Q.; Miao, Z.W.; Wang, R.; Yang, J.; Zhang, D.B. Hesperetin induces apoptosis in human glioblastoma cells via p38 MAPK activation. *Nutr. Cancer* **2020**, *72*, 538–545. https://doi.org/10.1080/01635581.2019.1638424.
57. Jo, S.H.; Kim, M.E.; Cho, J.H.; Lee, Y.; Lee, J.; Park, Y.-D.; Lee, J.S. Hesperetin inhibits neuroinflammation on microglia by suppressing inflammatory cytokines and MAPK pathways. *Arch. Pharm. Res.* **2019**, *42*, 695–703. https://doi.org/10.1007/s12272-019-01174-5.
58. Lu, C.; Yang, W.; Chu, F.; Wang, S.; Ji, Y.; Liu, Z.; Yu, H.; Qin, S.; Sun, D.; Jiao, Z.; et al. Hesperetin attenuates T-2 toxin-induced chondrocyte injury by inhibiting the p38 MAPK signaling pathway. *Nutrients* **2024**, *16*, 3107. https://doi.org/10.3390/nu16183107.
59. Gu, R.; Zhao, F.; Li, Q.; Hou, L.; Liu, G.; Sun, X.; Du, J.; Fang, B. Hesperetin inhibits porcine reproductive and respiratory syndrome virus replication by downregulating the P38/JUN/FOS pathway in vitro. *Microorganisms* **2025**, *13*, 450. https://doi.org/10.3390/microorganisms13020450.
60. Cuijpers, I.; Dohmen, C.G.M.; Bouwman, F.G.; Troost, F.J.; Sthijns, M.M.J.P.E. Hesperetin but not ellagic acid increases myosin heavy chain expression and cell fusion in C2C12 myoblasts in the presence of oxidative stress. *Front. Nutr.* **2024**, *11*, 1377071. https://doi.org/10.3389/fnut.2024.1377071.

Disclaimer/Publisher's Note: The statements, opinions and data contained in all publications are solely those of the individual author(s) and contributor(s) and not of MDPI and/or the editor(s). MDPI and/or the editor(s) disclaim responsibility for any injury to people or property resulting from any ideas, methods, instructions or products referred to in the content.